Transient gratings and second-harmonic probing of the phase transformation of a GaAs surface under femtosecond laser irradiation

S. V. Govorkov
Physics Department and International Laser Center, Moscow State University, Moscow 119 899, Russia

Th. Schröder
Institut für Optik und Quantenelektronik, Friedrich-Schiller-Universität, O-6900 Jena, Federal Republic of Germany

I. L. Shumay
Physics Department and International Laser Center, Moscow State University, Moscow 119 899, Russia

P. Heist
Institut für Optik und Quantenelektronik, Friedrich-Schiller-Universität, O-6900 Jena, Federal Republic of Germany
(Received 30 January 1992)

Using a transient-grating diffraction technique, we have compared the ultrafast dynamics of the linear reflectivity from a GaAs surface at the fundamental and second-harmonic frequencies with the dynamics of the second-harmonic generation (SHG) in reflection at an excitation level exceeding the melting threshold. It is shown that the ultrafast (within 100 fs) drop in the SHG efficiency cannot be accounted for by changes in the linear dielectric susceptibility that take place on a longer time scale. This fact indicates a fast change of the long-range crystalline symmetry of GaAs within a semiconductorlike phase, preceding a transition to the metallic phase as the crystal is melted.

INTRODUCTION

Ultrafast dynamics of optical reflection from semiconductor surfaces due to a laser-induced phase transition is of great current interest. Nonlinear reflection is of particular interest since the nonlinear optical susceptibilities are known to be directly related to crystal lattice symmetry. In particular, the second-order dipole-type nonlinearity $\chi^{(2)}$, which is allowed in noncentrosymmetric semiconductors (like GaAs), vanishes in a melted or disordered material. In the case of centrosymmetrical semiconductors (Si, Ge), a well-pronounced anisotropy of the quadrupole-type $\chi^{(2)}$ can be employed for structure-sensitive measurements.

Several research groups have reported measurements of the ultrafast dynamics of the reflected second harmonic (SH) from Si and GaAs during femtosecond pulsed laser irradiation which exceeds the melting threshold.[1–7] Tom, Aumiller, and Brito-Cruz[2] pointed out that variation of the anisotropic part of $\chi^{(2)}$ in Si occurs on a time scale of 100 fs, which is close to the optical phonon oscillation period and is much shorter than the carrier-lattice energy-transfer time. This conclusion leads to the hypothesis of "cold melting" of the lattice. An ultrafast decrease of the SH intensity from GaAs on a time scale of 100 fs was observed in Refs. 3–7. These data seem to indicate a fast carrier-driven structural transition, with the lattice temperature remaining well below the melting point. Sokolowski-Tinten *et al.*[7] reported that as the pump-pulse fluence became larger, the response times of reflectivity and SH shortened down to a 100-fs scale. A similar tendency was also noticed by Saeta *et al.*[4] Thus, the conclusion was made that fast carrier-induced processes play an important role in phase transitions at a laser fluence several times that of the melting threshold. On the other hand, ordinary melting can account for the observed, relatively slow changes just above the melting threshold.

We reported recently[6] that the characteristic time of the variation of a symmetry-dependent parameter (SH intensity) in GaAs is several times less than that of symmetry-independent linear reflection, similar to the case of Si.[2] This observation was interpreted in terms of a carrier-assisted transition to a nonequilibrium semiconductorlike phase preceding melting.[6,8] However, the direct comparison of linear and nonlinear reflections is complicated since the reflected SH intensity is governed by a number of factors. First, the escape depths at the fundamental laser frequency (wavelength 620 nm) and at the SH frequency differ by at least an order of magnitude. Second, a change of the SH intensity might in principle be caused by variations of the linear dielectric constants at ω and 2ω (the latter has not yet been studied). Finally, the effects of "saturation" and "screening" of $\chi^{(2)}$ by free carriers cannot simply be ignored.

In the present work, we employed the technique of transient gratings to study, with an improved signal-to-noise ratio, the dynamics of the linear optical properties of the GaAs subsurface layer, following the above-mentioned melting-threshold excitation with 100-fs laser pulses. The main purpose of this study was to compare the dynamics of the optical constants at the fundamental laser frequency ω and the second-harmonic frequency 2ω with the dynamics of second-harmonic generation in

reflection, in order to elucidate possible effects of the variation of linear optical properties on the second-harmonic generation (SHG) and thereby extract information on *structural* changes directly related to the nonlinear optical susceptibility of the subsurface layer. It was observed that the reflectivity both at ω and at 2ω exhibits relatively slow (on a time scale of 0.5 ps) changes, as compared with an abrupt (100-fs) drop in the SHG intensity. Numerical modeling based on solving the Helmholtz equation in the subsurface layer which accurately takes into account spatiotemporal variations of both linear and nonlinear optical constants proved that the variation of the linear optical constants alone cannot account for the observed ultrafast decrease in the SHG intensity. Therefore, an abrupt drop in SHG within 100 fs implies a structural phase transition other than melting.

EXPERIMENT

A standard colliding-pulse mode-locked (CPM) laser followed by a four-stage excimer-laser-pumped amplifier was used as a source of 0.1-mJ, 100-fs pulses at 620 nm. The experimental geometry is shown schematically in Fig. 1. Two pump pulses of approximately equal energy created a grating on the surface of the sample, provided that their temporal and spatial overlap was ensured. A weak probe pulse at 620 nm with energy $\frac{1}{60}$ that of the pump energy and an even weaker probe pulse at 310 nm were focused onto the central part of the illuminated area at the angle of incidence of 60°. The probe pulse at doubled frequency was generated by passing thin (< 1-mm) $LiIO_3$ crystal and both pulses at ω and 2ω were focused onto the sample surface by a concave aluminum mirror in order to ensure their temporal overlap. Undesirable effects of coherent interaction of pump and probe pulses[6] can be suppressed by a proper choice of the polarizations. In our experiment here, both pump pulses at ω were *s*-polarized, while the probe pulse at ω was *p*-polarized and that at 2ω was *s*-polarized. Measurements of diffraction of probe pulses at ω and 2ω were performed in one and the same series of experiments, and measurements of SH were carried out separately under the same conditions in order to get rid of stray light from the probe radiation at 2ω.

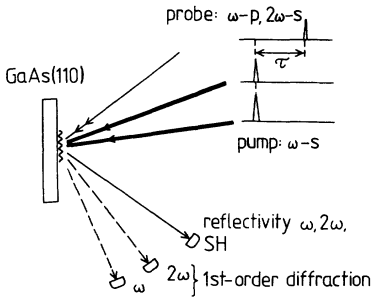

FIG. 1. Schematic diagram of experimental configuration. Two pump pulses with *s*-polarizations at frequency ω overlap both in time and space at the sample surface. The coinciding probe pulses at ω and 2ω are *p*- and *s*-polarized, respectively. The SHG intensity, linear reflectivity at ω and 2ω and the first-order diffraction efficiency at ω and 2ω [denoted in the text as $D(\omega)$ and $D(2\omega)$, respectively] are registered.

The sample used was a GaAs(110) wafer processed with use of a standard polishing procedure. It was moved in plane by a stepping motor in order to ensure the irradiation of a fresh surface area by each subsequent laser pulse.

First, we measured the dynamics of the linear reflectivity at ω and 2ω with the pump-pulse fluence at the maxima of the interference pattern being four times that of the melting threshold (the fluence of each pump pulse alone was just at the melting threshold). The data of Fig. 2(b) show the behavior of the linear reflectivity at ω and 2ω on a longer time scale (about 10 ps). The dynamics of the reflectivity at ω qualitatively follows previous data.[4-7] The reflectivity at 2ω also demonstrates a fast rise during the first picosecond but the difference in reflectivity before and after the phase transition is several times lower, as one might expect. Another feature is the somewhat larger scatter of data at 2ω, most probably due to a higher sensitivity of the reflection at 2ω to surface inhomogeneity across the sample. Note also the gradual decrease in both $R(\omega)$ and $R(2\omega)$ at longer times caused by effects of evaporation, turbulence, etc., of the melted material. Again, this effect is more pronounced at 2ω because of a much smaller escape depth and, hence, higher surface sensitivity. Thus, one can conclude that the relatively large scattering of the data at 2ω does not allow an unambiguous determination of the $R(2\omega)$ rise time with accuracy sufficient to compare it with that of $R(\omega)$ and the decay time of SHG intensity.

In contrast, the intensity of the first-order diffracted pulses [Fig. 2(a)] demonstrate an excellent signal-to-noise ratio, thus making quantitative analysis possible. The decrease in R on a 10-ps time scale can be attributed to the increase of diffuse scattering. At the same time, the intensity of diffracted pulses continues to grow, thereby in-

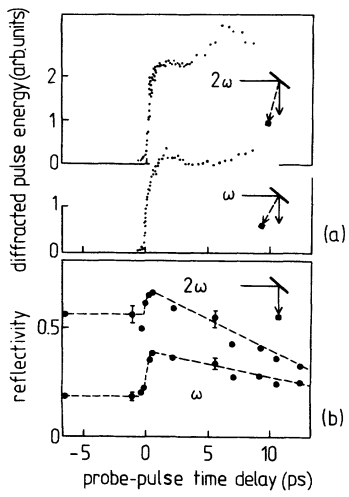

FIG. 2. First-order diffraction efficiency (a) and reflectivity (b) vs time delay of probe pulses. Dashed lines provide a guide for an eye. Note the difference in signal-to-noise ratio for reflectivity and diffraction.

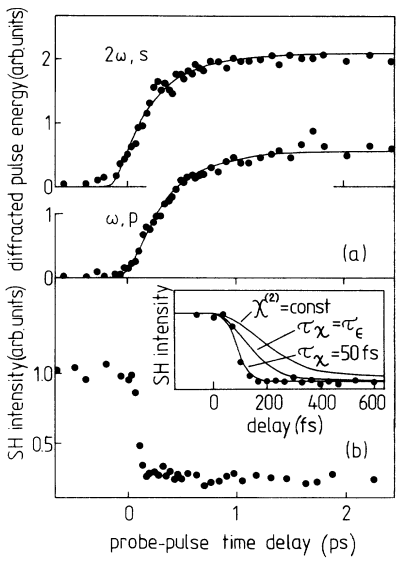

FIG. 3. Diffraction efficiency at ω and 2ω (a) as compared to SHG efficiency (b). The points represent experimental data, the smooth lines represent the theoretical fit explained in the text. The inset shows SHG dynamics within 1 ps. Theoretical fits assuming $\chi^{(2)}$=const, $\tau_\chi=\tau_\epsilon$, and $\tau_\chi=50$ fs are shown (see the text).

dicating a rise of the grating amplitude.

Figure 3 represents the dynamics of the first-order diffraction of the probe pulses at ω and 2ω, together with the SHG data at maximum laser fluence exceeding the melting threshold by a factor of 4. Both diffraction efficiencies $D(\omega)$ and $D(2\omega)$ demonstrate a fast rise within the first picosecond and a leveling off for at least a few picoseconds. The rise time of $D(2\omega)$ appears to be a little bit shorter but comparable to that of $D(\omega)$. In contrast, the SHG intensity exhibits an abrupt decrease within 150 fs followed by slower changes.

Both the observed differences in dynamics of $D(\omega)$ compared with those of $D(2\omega)$ and the observed differences in dynamics of D compared with that of the SHG should be explained. It seems reasonable that the former difference is caused by a difference in escape depths and by the frequency dispersion of the linear optical constants. Indeed, the escape depth at 2ω is less than that at ω (13 and 230 nm, respectively[9]) by more than one order of magnitude; thus, the reflected pulses at ω and 2ω are produced in layers of quite different thicknesses. Since the laser intensity decreases in the bulk, the characteristic time for a phase transition is expected to increase in the bulk, thus effectively slowing down the variation of the reflectivity at ω. On the other hand, whether the difference in Fresnel's factors for the linear and nonlinear reflection can account for the difference in the dynamics of diffraction efficiencies $D(\omega)$ and the SHG is not understood. To address these problems a numerical modeling, taking into account dynamics of depth profiles of linear and nonlinear constants should be performed.

NUMERICAL MODELING

The fast changes in the optical constant over a depth profile can be accurately taken into account by solving the Helmholtz equation. In this way, the effect of the change in the linear dielectric constants on the SHG intensity is simultaneously taken into account. The one-dimensional Helmholtz equation for a p-polarized incident pulse at ω can be written as

$$\frac{\partial^2 B_\omega}{\partial z^2}-\frac{1}{\epsilon_\omega}\frac{\partial \epsilon_\omega}{\partial z}\frac{\partial B_\omega}{\partial z}+k_0^2(\epsilon_\omega-\sin\theta)B_\omega=0 \tag{1}$$

and that for an s-polarized wave at 2ω as

$$\frac{\partial^2 E_{2\omega}}{\partial z^2}+4k_0^2(\epsilon_{2\omega}-\sin^2\theta)E_{2\omega}=0\ . \tag{2}$$

Here B and E are the magnetic- and electric-field vectors, respectively, which are parallel to the surface in each case, $\epsilon(z,t)=\epsilon_1+i\epsilon_2$ is the complex dielectric constant, z is the distance from the surface (negative direction is towards the bulk), k_0 is the wave number of the fundamental wave in vacuum, and θ is the angle of incidence. The initial conditions were specified at a depth of at least ten times the fundamental radiation absorption length and were calculated from (1) and (2) assuming $\epsilon(z)=\epsilon_{\text{cryst}}=$const and substituting a wave with wave number $k_0\epsilon^{1/2}$. The complex reflectivity coefficient $r=E_{\text{refl}}/E_{\text{inc}}$ was calculated by matching solution (1) or (2) to the solution of the wave equation for vacuum at the surface.

The periodic variation of the coefficient $r(y)$ across the surface forms the grating from which the probe beam is scattered. The intensity of the first-order diffracted beam is proportional to the modulus of the first Fourier component of $r(y)$ squared:[10]

$$D\propto\left|\int_{-\infty}^{+\infty} r(y)\exp[-ik_0(\sin\theta_{\text{diff}}-\sin\theta)y]dy\right|^2\ . \tag{3}$$

In order to calculate the reflected SHG intensity one should introduce the nonlinear source S_{NL} proportional to

$$S_{\text{NL}}\propto\frac{1}{\epsilon_2}\frac{\partial\epsilon_{2\omega}}{\partial z}j_y^{\text{NL}}+\frac{\partial j_z^{\text{NL}}}{\partial y}-\frac{\partial j_y^{\text{NL}}}{\partial z} \tag{4}$$

into the right side of Eq. (1) (rewritten for 2ω). Here the components of nonlinear current can be obtained using values of the electric field strength $E_\omega(z)$ calculated from (1) inside the crystal and the nonlinear susceptibility tensor $\hat{\chi}^{(2)}$:

$$\bar{j}_{\text{NL}}\propto\hat{\chi}^{(2)}(z,t):\bar{E}_\omega\bar{E}_\omega\ , \tag{5}$$

$$\bar{E}_\omega=(ic/\omega\epsilon)_\omega\nabla\times\bar{B}_\omega\ . \tag{6}$$

Zero initial conditions for (1) with a nonlinear source were assumed for the bulk. In this case, the solution appears to be a superposition of a generated SH wave and a free wave, which is the solution of (1) at 2ω without the source; therefore the free wave, which can be calculated as a product of the incident wave and $r(2\omega)$, must be subtracted from the solution to yield the actual generated SH wave. Finally, the total intensity of the SHG pulse was calculated by integrating the SH field strength over the surface grating and the probe pulse temporal shape. Of

interest is the dynamics of linear (ϵ) and nonlinear ($\chi^{(2)}$) susceptibilities, which in fact are free parameters in our model. First, we assume that ϵ changes in time *continuously* (exponentially) from its crystal (unpumped) values [$\epsilon(\omega)=14.99+i1.637$; $\epsilon(2\omega)=9.279+i13.832$] (Ref. 9) to the metallic values [$\epsilon(\omega)=-7.56+i22.8$; $\epsilon(2\omega)=-5.25+i50$],[11] thereby effectively taking into account the inhomogeneous nature of the phase transition. One should keep in mind that the observed transition occurs on an ultrashort time scale, therefore most likely via nucleation and subsequent growth of the melted volume. Thus, the layer which undergoes a transition into a new phase is certainly highly inhomogeneous and its average susceptibility cannot change abruptly.

The characteristic time of the transition τ depends on the laser intensity I_ω which decreases in the bulk:

$$I_\omega = I_{\omega 0} \exp(\alpha z) , \tag{7}$$

where $\alpha = 4.4 \times 10^4$ cm^{-1} is the absorption coefficient at ω and $I_{\omega 0}$ is the laser intensity at the surface. To take into account the observed decrease in the characteristic time of the phase transition as the laser fluence increases (see Ref. 7), we assume

$$\tau = \tau_\epsilon [(I_{\omega 0} - I_{\rm th})/(I_\omega - I_{\rm th})]^\delta , \tag{8}$$

where $I_{\rm th}$ is melting threshold intensity, and δ and τ_ϵ are free parameters. In fact, the value of δ governs the difference in rise times of $D(\omega)$ and $D(2\omega)$ since it determines the rate of change of τ towards the bulk. The variation of τ_ϵ influences both rise times in direct proportion; therefore it is possible to vary τ_ϵ and δ independently to fit the experimental data. We obtained a rather good fit with values $\tau_\epsilon = 300$ fs and $\delta = 1.0$ (with $I_{\omega 0}/I_{\rm th} = 4$)—see Fig. 3(a). As a matter of fact, variations of δ in the range 0.8–2.0 were required to change τ_ϵ by not more than 25% to restore a satisfactory fit to the data. On the other hand, the value of $\delta = 1.0$ is a rather good approximation of the data of Refs. 4 and 7 in the range of fluences up to four times the threshold value.

It should be noted that calculations of the reflectivity $R(\omega)$ revealed a well-known "dip" preceding the rise of $R(\omega)$.[4,7] This dip is caused by ϵ_1 becoming zero as it changes from an initially positive to large negative value characteristic of the molten phase. The diffraction of probe pulse at ω does not reveal such a dip because the diffraction efficiency is governed not only by the amplitude but also by the phase of reflection coefficient $r(y)$. It means that a grating can exist even if R is equal to its initial unpumped value. Nevertheless, the nonmonotonic variation of the reflectivity at ω causes slowing the rise of diffraction at ω as compared with diffraction at 2ω, because $R(2\omega)$ rises monotonically from the very beginning. The latter behavior is a consequence of $\epsilon_2(2\omega)$ being larger than $\epsilon_1(2\omega)$. This difference also contributes to the difference in diffraction dynamics at ω and 2ω.

Consider now the dynamics of the SHG in reflection. It is seen from Fig. 3 (inset) that even if the nonlinear susceptibility $\chi^{(2)}$ were equal to a constant, the efficiency of the SHG would still exhibit a decrease due to the variation in ϵ (e.g., decrease of the escape depth). If one assumes that $\chi^{(2)}$ decreases exponentially with the same characteristic time as that governing melting, then one obtains a somewhat faster decrease in the SH intensity (see Fig. 3). Note the difference in the rates of decrease in the SH and the rise of diffraction in these two cases, despite their similar origin. This fact is consistent with a simple estimate based on formulas for the SH generated under normal incidence (for simplicity) in reflection from a homogeneous medium with the dielectric susceptibility ϵ:[12]

$$I_{\rm SH} \propto P^2(2\omega) F^2(\theta, \epsilon_\omega, \epsilon_{2\omega}) . \tag{9}$$

Here the effective bulk polarization $P(2\omega)$ and Fresnel factor F can be evaluated as follows:

$$\begin{aligned} &P(2\omega) \propto R_\omega^{-1} , \\ &F \propto \epsilon_\omega^{1/2} (4\epsilon_{2\omega} - \epsilon_\omega)^{-1} (\epsilon_\omega^{1/2} + 1)^{-1} . \end{aligned} \tag{10}$$

It is seen that $I_{\rm SH}$ decreases faster than R^{-1} even if $\chi^{(2)} = {\rm const}$.

However, the rates obtained are still insufficient to account for the drop in the SH intensity observed experimentally. Therefore, the nonlinear susceptibility $\chi^{(2)}$ should change with a characteristic time *less* than that of ϵ. In particular, Fig. 3 shows a curve calculated with $\tau_\chi = 50$ fs, which approximates the experimental data much better. In this case, the decay time of the SH is determined mainly by the pulse duration.

Thus, the main conclusion of this section is that the fast drop in the SH intensity observed experimentally cannot be attributed entirely to variations of the linear susceptibility ϵ, although the latter also contributes to this drop. Therefore, the characteristic decay time of $\chi^{(2)}$ must be several times shorter than that of the linear dielectric permeability.

DISCUSSION

The observed response times of the dielectric constant ϵ ($\tau_\epsilon = 300$ fs) and the SHG ($\tau_\chi < 100$ fs) are at least an order of magnitude less than the photoexcited-carrier–lattice energy-transfer time. This fact is in agreement with previous data of Refs. 2–7. Several groups[2,4,6,7] concluded that such a transition must be electronic in nature, namely, occurring via a weakening of atomic bonds due to the presence of an ultradense ($N \cong 8 \times 10^{21}$ cm^{-3}) (Ref. 4) plasma of free carriers.

Let us consider in detail the difference in response times between the linear and nonlinear susceptibilities. A dipole-type second-order nonlinearity in GaAs at $\omega = 2$ eV is caused mainly by the nonlinear response of bound electrons. Therefore, several reasons might principally result in a decrease in $\chi^{(2)}$ in GaAs: (i) removing of electrons from their initial states in the valence band ("saturation" of $\chi^{(2)}$); (ii) screening of the ionic potential by a dense e-h plasma, leading to a change of its symmetry; (iii) a transformation of the atomic configuration, or a structural phase transition. The first two processes are purely electronic and, therefore, are characterized by an ultrafast response time. However, neither of them has any threshold; therefore one might expect their effect on

$\chi^{(2)}$ to change gradually with increasing plasma density and laser fluence. This prediction is in disagreement with the observed behavior of the SH as a function of the laser fluence.[4,7] Moreover, the saturation of interband transitions at ω and 2ω involved in $\chi^{(2)}(2\omega,\omega,\omega)$, as well as a change of the band structure in case (ii), should manifest itself in a variation of the linear reflectivity at ω and/or 2ω, which is not the case within the 100-fs observed response time of the SHG.

Thus, we come to the conclusion that the 100-fs drop in $\chi^{(2)}$ is caused mainly by the change in the atomic configuration. Since the linear dielectric response changes more slowly, the symmetry corresponding to the long-range order and governing $\chi^{(2)}$ is therefore subjected to a change *prior* to changes in the short-range coordination which is necessary for transformation of GaAs to the metal-like state with corresponding metallic linear optical parameters. In other words, GaAs remains semiconductorlike during the first 300 fs after excitation, while its long-range structure has been transformed to the centrosymmetrical state.

This centrosymmetrical semiconductorlike phase might be either disordered or crystalline. A principal possibility of ultrafast transition to a disordered phase can be illustrated with a simple estimate. The excess energy of amorphous semiconductors with diamondlike tetrahedral short-range coordination over crystalline ones can be estimated as a difference in latent heats between the crystalline and amorphous phases (neglecting the difference in melting temperatures which tends to decrease this value). For example, this difference amounts to 1.1 kJ/cm^3 for Si.[13] This value constitutes an upper limit on the excess energy which is stored in the lattice with lost long-range order. In our case the actual value of the excess energy should be lower because of the presence of the *e-h* plasma. The estimated energy is six times less than the latent heat of melting of crystalline Si (4.2 kJ/cm^3) (Ref. 13) plus the energy needed (2.4 kJ/cm^3) to heat Si from 300 K up to the melting point. It means that only a small part of the energy stored in the photoexcited plasma is needed before a disordered phase is reached (taking into account a factor-of-4 excess over the melting threshold). This amount of energy can be transferred to the lattice within the time an order of magnitude shorter than the time necessary to melt the semiconductor. Estimates of the nuclear thermal velocities at room temperature[4] also provide values sufficient for nuclei to move by more than 10% of the lattice parameter within 100 fs.

Another possibility is the transformation of GaAs to the ordered crystalline phase with centrosymmetric (orthorhombic) structure.[8] Ultrafast transition to this state could occur via an electronically driven coherent shift of nuclei to the quasiequilibrium positions in a new lattice.[8]

A complete understanding of the bulk symmetry transformations in the near-surface layer within 100 fs of laser excitation requires application of some other structure-sensitive technique, for example, x-ray, particle scattering, etc. However, these techniques lack the necessary time resolution.

CONCLUSION

In conclusion, comparing femtosecond dynamics of the linear optical response at the fundamental and doubled CPM-laser frequencies and the dynamics of the second-harmonic generation in reflection, we have shown that the top 13-nm-thick layer of GaAs transforms to the centrosymmetrical semiconductorlike phase existing over approximately 300 fs after the 100-fs laser excitation. This phase is followed by the state with a metallic linear optical response typical of a molten material.

ACKNOWLEDGMENTS

Helpful discussions with Professor N. I. Koroteev and Professor W. Rudolph are gratefully acknowledged.

[1]C. V. Shank, R. Yen, and C. Hirlimann, Phys. Rev. Lett. **51**, 900 (1983).

[2]H. W. K. Tom, G. D. Aumiller, and C. H. Brito-Cruz, Phys. Rev. Lett. **60**, 1438 (1988).

[3]T. Schroder, W. Rudolph, S. V. Govorkov, and I. L. Shumay, Appl. Phys. A **51**, 49 (1990).

[4]J. K. Wang, P. Saeta, Y. Siegal, E. Mazur, and N. Bloembergen, in *Ultrafast Phenomena VII,* edited by C. B. Harris, E. P. Ippen, G. A. Mourou, and A. H. Zewail, Springer Series in Chemistry and Physics Vol. 53 (Springer, Berlin, 1990), p. 321; P. Saeta, J.-K. Wang, Y. Siegal, N. Bloembergen, and E. Mazur, Phys. Rev. Lett. **67**, 1023 (1991).

[5]H. Schulz, J. Bialkowski, K. Sokolowski-Tinten, and D. von der Linde, in *Ultrafast Phenomena VII* (Ref. 4), p. 365.

[6]S. V. Gorokov, I. L. Shumay, W. Rudolph, and T. Schroder, Opt. Lett. **16**, 1013 (1991).

[7]K. Sokolowski-Tinten, H. Schulz, J. Bialkowski, and D. von der Linde, Appl. Phys. A **53**, 227 (1991).

[8]S. V. Govorkov, V. I. Emel'yanov, and I. L. Shumay, Laser Phys. **2**, 1 (1992).

[9]D. E. Aspnes and A. A. Studna, Phys. Rev. B **27**, 985 (1983).

[10]M. Born and E. Wolf, *Principles of Optics* (Pergamon, Oxford, 1964), Chap. 8.

[11]We used Drude parameters similar to those given in Ref. 7.

[12]Y. R. Shen, *The Principles of Nonlinear Optics* (Wiley, New York, 1984), Chap. 25.

[13]R. F. Wood and J. E. Jellison, Jr., in *Semiconductors and Semimetals,* Vol. 23 of *Pulsed Laser Processing of Semiconductors,* edited by R. F. Wood, C. W. White, and R. T. Young (Academic, Orlando, 1984), p. 166.